Proceedings of the 35th European Safety and Reliability & the 33rd Society for Risk Analysis Europe Conference
Edited by Eirik Bjorheim Abrahamsen, Terje Aven, Frederic Bouder, Roger Flage, Marja Ylönen
 Published by Research Publishing, Singapore.
doi: 10.3850/978-981-94-3281-3_ESREL-SRA-E2025-P2317-cd

Numerical Solution of the Fokker-Planck Equation for the Overflow Probability of a Radioactive Near Surface Repository by the Crank-Nicolson Method: Preliminary Results

A. C. M. Alvim[1], D. G. Teixeira[1], P. F. Frutuoso e Melo[1]

[1]*Graduate Program of Nuclear Engineering, COPPE, Federal University of Rio de Janeiro, Rio de Janeiro, RJ, Brazil, E-mails: alvim@nuclear.ufrj.br, dteixeira@nuclear.ufrj.br, frutuoso@nuclear.ufrj.br*

A. S. M. Alves[2]

[2]*Eletrobras Eletronuclear S.A., Rio de Janeiro, RJ, Brazil, E-mail: asergi@eletronuclear.gov.br*

In an earlier paper we discussed the analytical solution of the Fokker-Planck (FP) equation for evaluating the overflow probability for the near surface repository of Abadia de Goiás, Brazil. Some preliminary considerations were approached in this reference. However, a formal approach for validating the results needed to be formulated. In this sense, we face the problem in this paper by approaching the solution for the overflow probability by numerical methods. An implicit numerical method was used, namely, the Crank-Nicolson method, which is known to be numerically stable. A discussion is performed on the initial and boundary conditions to solve the FP equation in order to obtain the probability density needed for calculating the overflow probability (in this sense, contrary to the analytical solution, the numerical solution does not need to be truncated because it starts at $t = 0$ with the defined initial condition). This latter depends on the repository institutional control period and, as in earlier published work on this subject, the institutional control period is varied from 5 years to 60 years. This wide range variation interval is justified by the fact that the repository design considers initially an institutional control period equal to 50 years. The numerical results for the probability density agree in terms of magnitude orders with the analytical ones published earlier. The overflow probabilities obtained are in good agreement with the ones obtained by the analytical methods.

Keywords: Near surface repository, Abadia de Goiás, Overflow probability, Fokker-Planck equation, Crank-Nicolson method.

1. Introduction

After the Goiânia accident (IAEA, 1988), a near surface radioactive repository was designed and constructed in order to deposit the radioactive wastes contaminated with ^{137}Cs (Tranjan Filho et al, 1997). A whole set of parameters was identified and considered in the design.

In an earlier paper (Gabcan et al, 2023) we discussed the analytical solution of the Fokker-Planck (FP) equation for evaluating the overflow probability for the near surface repository of Abadia de Goiás, Brazil. Some preliminary considerations were approached in this reference. However, a formal approach for validating the results needed to be formulated. In this sense, we face the problem in this paper, by approaching the solution for the overflow probability by numerical methods.

We begin the discussion in section 2 by considering a literature review on the numerical solution of the FP equation. Section 3 is dedicated to the discussion both of the analytical and numerical solutions of the FP equation, where an overview of the analytical solution developed in Gabcan et al (2023) is presented, together with the numerical one, based on the Crank-Nicolson method (Neena et al, 2022). The methodology used for obtaining the numerical results is presented and discussed in section 4. Section 5 compares results obtained with the Crank-Nicolson time discretization to the analytical results of Gabcan et al (2023). It is important to stress that the comparison of the solutions is performed taking into account the overflow probability of the repository, not the probability densities obtained for calculating them. Finally, conclusions reached are presented in section 6.

2. Literature Review

We present in this section a brief literature review on the subject.

Fukushima et al (2002) discuss numerical solutions to the FP equation by using the finite difference method for a thermally assisted reversal of the magnetization in a single-domain particle for which a truncated Fourier series expansion can be an approximate solution. Also, an integral function is used to accurately solve the equation.

Sun & Kumar (2014) present a solution to high-dimensional stationary FP equations by using tensor decompositions and Chebyshev spectral differentiation and applications to separable and non-separable systems, linear and nonlinear systems, and systems with and without closed-form stationary solutions up to 10-dimensional state spaces.

A finite difference scheme for solving the nonlinear FP equation is proposed in Sepehrian & Radpoor (2015). The intent is to discretize spatial derivatives. Next, a cubic $C1$-spline collocation method is used for the time integration of the resulting nonlinear system of ordinary differential equations. The proposed method has second-order accuracy in space and fourth-order accuracy in time variables. The numerical results confirm its validity.

Huang et al (2020) discuss a new convergence analysis for a finite element in space numerical method published earlier for solving fractional FP equations in a given domain with general forcing (i.e., the forcing term is both time dependent and space dependent).

Butt (2022) presents a discussion on the characterization and numerical scheme to a control problem governed by a three-dimensional time-dependent FP equation. The approach controls the drift of the stochastic FP process so that the probability density function attains a specific configuration. Also, an FP control strategy for collective motion is investigated and first-order optimality conditions are presented. On staggered grids, the Chang–Cooper discretization scheme that ensures the positivity, second-order accuracy, and conservativeness to the FP equation is employed to the discretized state system. Numerical experiments presented show the efficiency of the proposed numerical scheme to FP control problems.

Neena et al (2022) present three techniques for the numerical solution of the FP equation for some cases (FP with constant or linear drift coefficient, the backward Kolmogorov equation and the non-linear FP equation): the semi-implicit Euler, implicit Euler, and Crank-Nicolson. Three examples are presented for which analytical and numerical solutions are compared and the numerical methods proved to be competitive against existing methods.

The review presented shows diverse applications of methods that show the relevance of using finite difference methods.

3. Analytical and Numerical Solutions

The FP equation numerically solved here has an advective term and a diffusive term and is known as the forward Kolmogorov equation, Gabcan et al (2023).

We briefly discuss the analytical solution of the FP equation here because the details can be found in Gabcan et al (2023). Section 3.1 presents the basics for the analytical solution of the FP equation and section 3.2 is dedicated to the details of the numerical approach based on the Crank-Nicolson method.

3.1. *Analytical solution of the FP equation*

The starting point is Gabcan et al (2023), where the FP equation was analytically solved to allow for obtaining the probability density $p(x,t)$ for the liquid height (x) in the repository and for a given institutional control period (t), which is reproduced here for convenience.

$$p(x,t) = \frac{exp\left(-\frac{1}{2}\frac{(t.A(x)+x-x_o)^2}{\frac{F_d^2}{n_1^2}t} + t\frac{dA(x)}{dx}\right)}{\sqrt{2\pi t\frac{F_d^2}{n_1^2}}} \quad (1)$$

where,

$$A(x) = ax^2 + bx + c$$

$$a = \frac{K_c}{n_1}\frac{b_1 + b_2}{L(b_1.b_2)}$$

$$b = \frac{K_c}{n_1 E}$$

$$c = \frac{1}{n_1}[K_c - F_d(p'_m + i'_r - e'_r - r')]$$

Table 1 gives details on all parameters of Eq. (1), Gabcan et al (2023).

Table 1. Description of the parameters of Eq. (1)

Symbol	Description
F_d	Degradation function of the repository ceiling (*dimensionless*)
n_1	Internal porosity of the repository (*dimensionless*)
b_1	Repository base width (*m*)
b_2	Repository base length (*m*)
E	Repository base thickness (*m*)
L	Repository wall thickness (*m*)
x	Height of the liquid column inside the repository (*m*)
x_o	Initial value of x (*m*)
p'_m	Average rainfall rate (*m*/*yr*)
e'_r	Evapotranspiration rate (*m*/*yr*)
i'_r	Irrigation rate (*m*/*yr*)
r'	Surface runoff (*m*/*yr*)
K_c	Hydraulic conductivity of concrete (*m*/*yr*)

In Eq. (1), $p(x,t)dx$ is the probability that the liquid height inside the repository is between x and $x + dx$ for a given institutional control period t (Feller, 1968).

The FP equation is a partial differential equation in statistical mechanics used to describe the time evolution of the probability density function of the velocity of a particle under the influence of drag forces and random forces, as is the case in Brownian motion (Reif, 2009). As discussed in Gabcan et al (2023), it is applicable to the behavior of the liquid height inside the repository under discussion here.

It is seen from Eq. (1) that $p(x,t)$ in a non-linear function that depends on several constants and on some rates.

It is necessary to check the normalization property of p(x,t) from Eq. (1), Gabcan et al (2023) because although $p(x,t)$ is a solution to the FP equation the domain of variable x is not necessarily restricted to non-negative values. The random variable X represents the liquid height inside the repository. We can have a mathematical solution to the equation that not necessarily is a physical solution, so to get a physical solution, it is necessary to check the normalization condition of $p(x,t)$ (Feller, 1968). The probability density must be restricted to positive values of the liquid height and a physical upper limit must also be defined because no infinite heights are physically possible. From Alves et al (2015), an upper limit equal to 15 *m* has been adopted.

The value equal to 4.38 m is the average internal height of the concrete structure of the Abadia de Goiás Repository (Tranjan Filho et all, 1997), which is considered in the analysis. This value was obtained in the design of this repository, setting the values of the length and width of the base of the facility and using the volume of waste to be deposited. In the modeling presented in this article, it is considered that the repository overflow will occur for a liquid column height equal to or greater than that mentioned above.

The boundary conditions for the initially obtained $p(x, t)$ for which x can be negative is such that $p(-\infty, t) = p(+\infty, t) = 0$ [in this sense, it is advisable to check Fig. 3 of Gabcan et al (2023)]. On the other hand, $p(x, 0)$ is defined by means of a Dirac delta [see Eq. (12) of Gabcan et al (2023)].

In this sense, the normalization property means that:

$$\int_{10^{-4}}^{15} p(x,t)\,dx = \eta \qquad (2)$$

The overflow probability is obtained from:

$$P(X > 4.38; t) = \int_{4.38}^{15} \frac{p(x,t)}{\eta} dx \qquad (3)$$

$P(X > 4.38;t)$ means the probability that the liquid height is at least equal to 4.38 *m* (the repository height) for a given institutional control period, *t*.

3.2. *Numerical solution of the FP equation*

The FP equation describing the repository problem is a 2nd order parabolic partial differential equation in the given (x,t) domain. It comprises both an advective term and a diffusive term. To select an appropriate numerical method, it is essential to initially determine which term prevails over the other. Therefore, evaluating the Péclet number (Pe) through the domain is crucial for choosing a suitable numerical approximation. Pe quantifies the ratio between convective and diffusive effects: if $Pe \ll 1$, diffusion dominates, whereas if $Pe > 1$, convection is the primary influencing factor in the solution. The Péclet number was computed for various values of h_x, confirming that diffusion dominates across the entire x-domain. This justifies our choice of the numerical method described in this section (Anderson et al, 2021).

Also, in order to establish appropriate values for h_x and h_t, the Courant-Friedrichs-Levy (CFL) criterion was satisfied for the numerical mesh used. This criterion guarantees that in the time interval h_t the distance traveled by the wave or the information is not greater than the mesh space h_x. Although for the Crank-Nicolson time discretization adopted here, the CFL condition is not important to assure stability, it may influence the precision for larger time intervals (Anderson et al, 2021).

In order to discuss the numeric solution of the FP equation, we reproduce it here:

$$\frac{\partial p}{\partial t} = -\frac{dA(x)}{dx}.p - A(x)\frac{\partial p}{\partial x} + \frac{1}{2}\left(\frac{F_d}{n_1}\right)^2 \frac{\partial^2 p}{\partial x^2} \quad (4)$$

where $p = p(x,t)$ and $A(x)$ is defined as for Eq. (1).

A time discretization was performed, where the first-order partial derivative in time was approximated by forward differences, and the RHS of Eq. (4) was handled using the well-known Crank-Nicolson method (Richtmeyer & Morton, 1967). This space-time discretization is the same as used in Neena et al (2022), where both the spatial and time discretizations are referred to as the Crank-Nicolson scheme.

To facilitate the derivation of the numerical method applied to Eq. (4), the coefficients were redefined as:

$$coefp(x,t) = -(2ax + b)$$

$$coefdp(x,t) = -(ax^2 + bx + c)$$

$$coefd2p(x,t) = \frac{1}{2}\left(\frac{F_d^2}{n_1^2}\right)$$

Considering the spatial grid given by h_x and the time grid given by h_t, one arrives at:

$$beta_i p_i^{n+1} + delta_i p_{i+1}^{n+1} + alfa_i p_{i-1}^{n+1} = beta_e p_i^n + delta_e p_{i+1}^n + alfa_i p_{i-1}^n \quad (5)$$

where:

$$beta_i = 1 - \frac{h_t}{2} coefp_i + \frac{h_t}{h_x^2} coefd2p_i$$

$$delta_i = -\left(\frac{h_t}{4h_x} coefdp_i + \frac{h_t}{2h_x^2} coefd2p_i\right)$$

$$alfa_i = \frac{h_t}{4h_x} - \frac{h_t}{2h_x^2}$$

$$beta_e = 1 + \frac{h_t}{2} coefp_i - \frac{h_t}{h_x^2} coefd2p_i$$

$$delta_e = \left(\frac{h_t}{4h_x} coefdp_i + \frac{h_t}{2h_x^2} coefd2p_i\right)$$

$$alfa_i = -\frac{h_t}{4h_x} coefd2p_i + \frac{h_t}{2h_x^2} coefd2p_i$$

Eq. (4) results in a tridiagonal matrix system, which is then solved using the well-known tridiagonal matrix algorithm (TDMA).

After obtaining the numerical probability density with the help of Eq. (4), it is necessary to check its normalization property. The starting point for the liquid height is $x_o = 10^{-4}$ m (Table 2), for which the probability density is set equal to zero.

4. Methodology

The results are to be obtained for t = 5, 10, 20, 30, 40, 50, and 60 years. These values represent possible institutional control periods including the one considered in the repository design (Tranjan et al, 1997), that is, 50 *yr*.

The result that is of interest is the overflow probability, so that after obtaining the probability density from Eq. (1), one obtains this probability from Eq. (3) and this probability will be the parameter for comparison purposes.

For obtaining the analytical results, the starting point is also Eq. (1). It is necessary to take into account the design values for the parameters displayed in Table 1.

Table 2 displays the necessary data for the analysis (Gabcan et al, 2023).

Table 2. Design values for the parameters of Eq. (1) [Gabcan et al, 2023)]

Parameter	Design value
F_d	0.10 (*dimensionless*)
n_1	0.09 (*dimensionless*)
b_1	60 *m*
b_2	20.1 *m*
E	0.20 *m*
L	0.20 *m*
x_o	10^{-4} *m*
p'_m	1.592 *m/yr*
e'_r	1.457 *m/yr*
i'_r	1.592×10^{-2} *m/yr*
r'	1.5092×10^{-3} *m/yr*
K_c	3.15×10^{-4} *m/yr*

Notice that with the help of Table 2 and Eq. (3) it is possible to obtain all the needed analytical results.

On the other hand, for obtaining the numerical results, the starting point is Eq. (4). It is necessary to define a spatial grid. By performing some preliminary tests, the spatial grid was defined as follows: $h_x = 0.25\ m$ and $h_t = 10^{-4}\ yr$.

5. Results and Discussion

The results in Figures 1 – 7 were obtained for repository liquid heights varying from $10^{-4}\ m$ to 15 *m*. This height range is discussed in Frutuoso e Melo (2023). The truncated analytic solution for this case can be seen in detail in Gabcan et al (2023).

As mentioned earlier, the analysis begins with the consideration of the probability density for an institutional time period equal to 5 *yr*. In an earlier paper (Gabcan et al, 2023) we obtained the analytical probability density for this time period, named $p(x,5)$. It was evaluated by considering the discussion in section 3.1. Now, by applying the methodology discussed in section 4, it is possible to obtain this probability density by the Crank-Nicolson method.

Fig. 1 displays the results for the institutional control period of 5 *yr*.

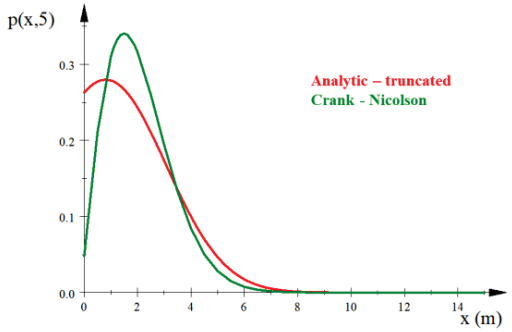

Fig. 1. Probability densities for an institutional control period of 5 years

If one considers the Crank – Nicolson solution (in green), it is seen that the curve peak is slightly drifted to the right and higher than the truncated analytic solution. The curves go to zero mainly for liquid heights higher than 6 *m*. The analytical curve starts at about 0.26, while the numerical one starts at about 0.05 (for $x = 10^{-4}\ m$).

There is quite a reasonable agreement between the truncated analytical solution and the Crank – Nicolson numerical solution, although the truncated analytic curve presents a peak at a liquid height around 0.7 m, while the numeric one presents a peak about 2 m.

It is clearly seen from Fig. 1 that the overflow probability evaluated from the analytical solution is higher than the one calculated from the numerically obtained probability density. The overflow probability obtained from the analytical probability density is equal to 8.16×10^{-2}, while the one obtained from the numerical solution for the FP equation is equal to 4.32×10^{-2}. It should be noted here that the calculation of this overflow probability involves calculating the area of the probability density $p(x,5)$ between 4.38 m and the liquid height limit, assumed to be 15 m. Also, if one calculates this overflow probability by considering a liquid height equal to infinity the difference is not significant because the probability density curves fall off to zero quite quickly.

The next step is to consider the numerical solution for $t = 10\ yr$. Fig. 2 displays the results for this case.

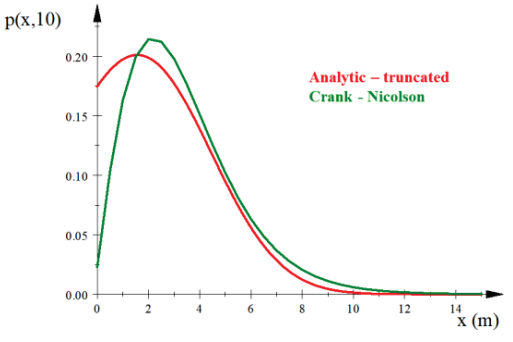

Fig. 2. Probability densities for an institutional control period of 10 years

As expected, the analytical solution drifts to the right with a peak lower than the one in Fig. 1. A better agreement is seen between the truncated analytical solution and the numerical solution, as compared to the results for the 5-year control period. Both curves flatten a little due to the diffusion-convection process. Both solutions approach the steady-state behavior.

Here, $p(0, 10) = 0.175$ (analytical solution) and $p(0, 10) = 0.025$ (numerical one). Both are smaller than for $t = 5\ yr$.

The overflow probabilities in this case are given by 2.14×10^{-1} for the truncated analytical solution (red), and 2.56×10^{-1} for the numerical solution (green). The numerical result is conservative although it retains the same order of magnitude of the analytical solution.

Fig. 3 displays the results for the institutional control period of 20 years.

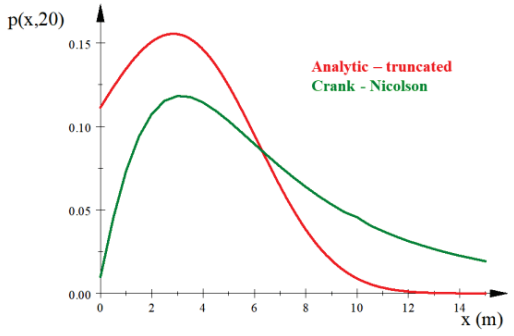

Fig. 3. Probability densities for an institutional control period of 20 years

The solution drift to the right goes on as the curves flatten and it is clear that the truncated analytical solution falls down faster than the numerical one. The numerical solution falls down much more slowly than the truncated analytical one. Notice also that the peaks of the numerical and steady-state solutions are quite closer (3 *m*). Even for a liquid height equal to 15 m, the numerical solution falls down slowly.

Also, $p(0, 20) = 0.1125$ (analytical) and $p(0, 20) = 0.015$ (numerical), so that this value is lower for the first case but remains constant for the second one as compared to those for $t = 10$ yr.

For this case, the overflow probability behaves as follows. It is equal to 3.73×10^{-1} (truncated) and 5.83×10^{-1} (numerical). Notice that the overflow probability in this latter case raises by a factor of over 50% in comparison to the result for the 10-year control period. This shows that the numerical solution is quite sensitive to institutional control periods between 10 *yr* and 20 *yr*.

Fig. 4 displays the results for the institutional control period equal to 30 *yr*.

The curves cross at about 7.2 *m* and their peaks are at about 4 *m* (analytical) and 3.5 *m* (numerical). Also in this case, the numerical probability density falls down to zero quite slowly (while the analytical approaches zero at about 13 *m* of liquid height). $p(0, 30) = 0.035$ (analytical) and $p(0, 30) = 0.0085$ (numerical), thus keeping the descending pattern.

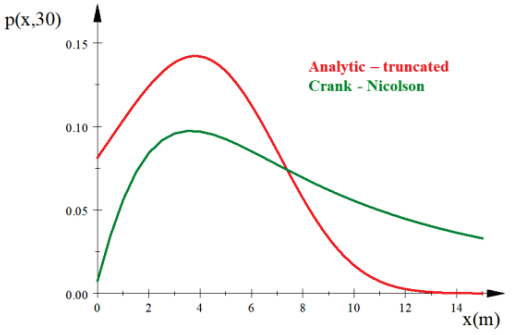

Fig. 4. Probability densities for an institutional control period of 30 years

Regarding the overflow probability, it is 4.67×10^{-1} (analytical) and 6.67×10^{-1} (numerical). Still in this case, the result for the numerical calculation is higher than the one for the analytical case. However, they still preserve the same order of magnitude.

Also, in this case the analytical solution starts at a value higher than the one for the numerical case.

Fig. 5 presents the results for $t = 40$ *yr*.

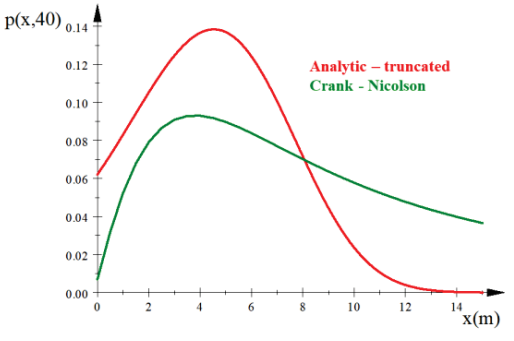

Fig. 5. Probability densities for an institutional control period of 40 years

The curve peaks are at about 4.5 *m* (analytical) and 3 *m* (numerical) and $p(0, 40) = 0.06$ (analytical) and $p(0, 40) = 0.01$ (numerical). The same curve pattern is preserved.

Concerning the overflow probability, it is 5.34×10^{-1} (analytical) and 6.85×10^{-1} (numerical) and the latter is still higher than the first one.

The next case to be presented and discussed

relates to the institutional control period of 50 years, which is the one chosen by the regulatory body, as mentioned earlier. Fig. 6 displays the results obtained.

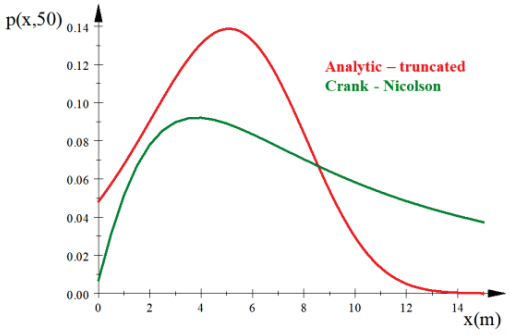

Fig. 6. Probability densities for an institutional control period of 50 years

It can be seen that the truncated analytical solution drifts to the right once again, as expected. Its peak is at about $x = 5$ *m* (analytical) and $x = 3$ *m* (numerical). On the other hand, the peak of the numerical solution is quite to the left and this numerical solution is practically the same as that for the 20-year institutional control period. Once again, the analytical solution falls off to zero much faster than the numerical one.

The overflow probabilities for this institutional control period are as follows. For the truncated analytical solution, it is equal to 5.88×10^{-1}. For the numerical solution, it is equal to 6.89×10^{-1}. Once again, the probability for the numerical solution is conservative and still about 50% higher than the one for the truncated analytical solution.

Fig. 7 presents the results for the last case envisaged, that for $t = 60$ *yr*.

It can be seen that $p(0, 60) = 0.045$ (analytical) and $p(0, 60) = 0.01$ (numerical). Notice that for the analytical case it keeps the descending pattern while for the numerical solution it is in the steady-state behavior. The peaks are at $x = 5.5$ *m* (analytical) and $x = 8.5$ *m* (numerical).

It can be seen that $p(0, 60) = 0.045$ (analytical) and $p(0, 60) = 0.01$ (numerical). Notice that for the analytical case it keeps the descending pattern while for the numerical solution it is in the steady-state behavior. The peaks are at $x = 5.5$ *m* (analytical) and $x = 8.5$ *m* (numerical).

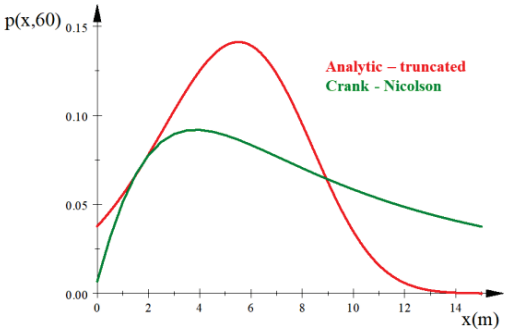

Fig. 7. Probability densities for an institutional control period of 60 years

Concerning the overflow probability, it is equal to 6.34×10^{-1} (analytical) and 6.90×10^{-1} (numerical). The numerical results reached the steady-state value at this point.

Table 3. Overflow probability: comparison and relative errors

t (*yr*)	Analytical	CN(*)	e (%)(**)
5	8.16×10^{-2}	4.32×10^{-2}	47.1
10	2.14×10^{-1}	2.56×10^{-1}	19.6
20	3.73×10^{-1}	5.83×10^{-1}	56.3
30	4.67×10^{-1}	6.67×10^{-1}	42.8
40	5.34×10^{-1}	6.85×10^{-1}	28.3
50	5.88×10^{-1}	6.90×10^{-1}	17.2
60	6.34×10^{-1}	6.90×10^{-1}	8.8
70	6.73×10^{-1}	6.90×10^{-1}	2.5
80	7.08×10^{-1}	6.90×10^{-1}	2.5

(*) CN = Crank-Nicolson
(**) e = relative error

Table 3 displays the results obtained for the overflow probability up to 80 *yr*. The inclusion of times greater than 60 *yr* is to show how the analytical solutions behave as compared with the numerical one (in what regards the steady-state behavior). It is seen that the highest relative error is obtained for t = 20 *yr*. For the design institutional control period of 50 *yr*, this error is equal to 17.2%.

Table 3 shows that the best results are those for $t = 70$ *yr* and 80 *yr* because the analytical solution reaches the steady-state behavior slower than the numerical one.

To obtain the numerical results each run of the program written in Fortran takes a few seconds to generate the results on a Dell EVO laptop with an i7 processor.

6. Conclusions

The purpose of this paper was to show that the analytical solution to the FP equation is validated by means of a numerical approach based on the Crank-Nicolson technique. The leading reference for this choice was Neena et al (2022).

The comparison of results for the design institutional control period of 50 *yr* showed that the relative error is about 17% for the overflow probability. Slightly higher values bring a better agreement between both solutions.

There is an oscillation in the relative error for small institutional control periods (5 yr – 20 yr) followed by a monotone decrease of this error up to an institutional control period of 80 yr. The best result is achieved for an institutional control period of 70 yr.

The results agree quite well if one considers their order of magnitude (mostly 10^{-1}). For the CN method an asymptotic value of 6.90×10^{-1} is reached while for the analytical solution it is slightly higher ($\sim 7 \times 10^{-1}$).

Acknowledgements

Two of the authors (ACMA, PFFM) would like to acknowledge their support from the Brazilian National Council for Scientific and Technological Development (CNPq) through grant 406822/2022-0. PFFM would also like to acknowledge his support from CNPq through grant 311911/2023-4 and Rio de Janeiro State Research Support Foundation (FAPERJ) through grant E-26/204.363/2024 (299910). Another author (DGT) would also like to acknowledge her support from FAPERJ through grant E-26/203.489/2023 (294149).

References

Alves, A. S. M., Frutuoso e Melo, P. F., Passos, E. M. (2015). Stochastic and deterministic models to evaluate the critical distance of a near surface repository for the dispose of intermediate and low-level radioactive wastes. *Nucl. Eng. Des.*, 287, 57–67.

Anderson, D. A, Tannehill, J. C., Pletcher, R. H., Munipalli, R., Shankar, V. (2021). *Computational Fluid Mechanics and Heat Transfer*, CRC Press, Boca Raton, FL.

Butt, M. M. (2022). Numerical solution to the 3D bilinear Fokker-Planck control problem, *Int. J. Comp. Math.*, 99-12, 2466-2481.

Feller, W. (1968). *An Introduction to Probability Theory and its Applications*, Wiley, New York, vol. 1.

Frutuoso e Melo, P. F., Teixeira, D. G., Alves, A. S. M. (2023). The role of physical parameters in the overflow probability of a radioactive near surface repository for low & intermediate level wastes: the case of Abadia de Goiás In: M. P. Brito, T. Aven, P. Baraldi, M. Cepin, E. Zio (Eds.), *Proceedings of the 33rd European Safety and Reliability Conference*, pp. 1454–1461. Research Publishing, Singapore.

Fukushima, H., Uesaka, Y., Nakatani, Y., Hayashi, N, (2002). Numerical solution of the Fokker-Planck equation by the finite difference method for the thermally assisted reversal of the magnetization in a single-domain particle, *J. Magnetism & Magnetic Materials*, 242-245, 1002-1004.

Gabcan, L., Alves, A. S. M., Da Silva, F. C., Teixeira, D. G., Frutuoso e Melo, P. F., 2023, Evaluation of the overflow probability from the Abadia de Goiás repository by the Fokker – Planck equation using the Trotter's formula, *Nucl. Eng. Des.*, 413, 112493.

Huang, C., Le, K. N., Stynes, M. (2020). A new analysis of a numerical method for the time-fractional Fokker-Planck equation with general forcing, *IMA J. Num. Anal.*, 40, 1217-1240.

IAEA (1988). *The Radiological Accident in Goiânia*, International Atomic Energy Agency, STI / PUB / 815, Vienna, Austria.

Neena, A. S., Mkhope, D. P. C., Awasthi, A. (2022). Some Computational Methods for the Fokker – Planck Equation, *Int. J. Comput. Math*, 8, 261.

Reif, F. (2009). Fundamentals of Statistical and Thermal Physics, Waveland, Long Grove, IL.

Richtmeyer, R. D., Morton, K. W. (1967). *Difference Methods for Initial Value Problems*, Interscience Publishers, New York, NY.

Sepehrian, B., Radpoor, M. K. (2015). Numerical solution of the non-linear Fokker-Planck equation using finite differences method and the cubic spline functions, *App. Math & Comp.*, 162, 187-190.

Sun, Y., Kumar, M. (2014). Numerical solution of the high dimensional stationary Fokker-Planck equations via tensor decomposition and Chebyshev spectral decomposition, *Comp. & Math. with Appl.*, 67, 1960-1977.

Tranjan Filho, A., Alves, A.S.M., Santos, C.D.P., Passos, E.V., Coutinho, F.P.M. (1997). Repository of Radioactive Cesium Waste - Abbey of Goiás Conception and Design (*in Portuguese*), https://www.ipen.br/biblioteca/cd/go10anosdep/Cnen/doc/manu20.pdf, accessed Sep 2024.